



3D-DIVIMP-HC modeling analysis of methane injection into DIII-D using the DiMES porous plug injector

Y. Mu^{a,*}, A.G. McLean^a, J.D. Elder^a, P.C. Stangeby^a, B.D. Bray^b, N.H. Brooks^b, J.W. Davis^a, M.E. Fenstermacher^c, M. Groth^c, C.J. Lasnier^c, D.L. Rudakov^d, J.G. Watkins^e, W.P. West^b, C.P.C. Wong^b

^a University of Toronto Institute for Aerospace Studies, 4925 Dufferin St., Toronto, Canada M3H 5T6

^b General Atomics, P.O. Box 85608, San Diego, CA 92186-5608, USA

^c Lawrence Livermore National Laboratory, P.O. Box 808, Livermore, CA 94550, USA

^d University of California-San Diego, 9500 Gilman Dr., La Jolla, CA 92093-0417, USA

^e Sandia National Laboratories, P.O. Box 5800, Albuquerque, NM 87185, USA

ARTICLE INFO

PACS:
28.52.Av
52.40.Hf
52.65.Pp

ABSTRACT

A self-contained gas injection system for the Divertor Material Evaluation System (DiMES) on DIII-D, the porous plug injector (PPI), has been employed for in situ study of chemical erosion in the tokamak divertor environment by injection of CH₄ [A.G. McLean et al., these Proceedings]. A new interpretive code, 3D-DIVIMP-HC, has been developed and applied to the interpretation of the CH, CI, and CII emissions. Particular emphasis is placed on the interpretation of 2D filtered-camera (TV) pictures in CH, CI and CII light taken from a view essentially straight down on the PPI. The code replicates sufficient measurements to conclude that most of the basic elements of the controlling physics and chemistry have been identified and incorporated in the code-model.

© 2009 Elsevier B.V. All rights reserved.

1. Introduction

Carbon plasma-facing surfaces in tokamaks are subject to chemical erosion due to hydrocarbon formation. Laboratory measurements of erosion yields cannot be applied with full reliability to tokamaks due to various tokamak-specific mechanisms, such as the prompt redeposition of hydrocarbon fragments. Understanding chemical erosion and molecular breakup in current tokamaks is important for making projections of tritium inventory in ITER due to codeposition. This understanding can be developed by applying models of hydrocarbon breakup and transport to the interpretation of spectroscopic observations of emissions resulting from hydrocarbons entering the plasma. This task was made easier by the development of a gas injection system on DIII-D which can simulate chemical sputtering by introducing a known quantity of hydrocarbon gas.

A Porous graphite Plug gas Injector (PPI) was developed by McLean et al. [1] for use with the Divertor Material Evaluation System (DiMES). The objective is to admit methane (or other hydrocarbon gases) through a porous graphite surface, so that the molecular interaction with the plasma closely approximates a hydrocarbon molecule released from a carbon surface by chemical

erosion. Injecting methane at a known rate provides direct calibration of spectroscopic signals from the Multichord Divertor Spectrometer (MDS) and the DiMES TV camera which view DiMES from above. The porous surface is designed such that size and spacing of the holes [~ 1000 holes, 0.25 mm (0.010 in.) diameter, 0.8 mm (0.032 in.) spacing] is on the order of the mean-free-path of CH₄ in an attached divertor plasma. The holes comprise <10% of the surface area so that the probe closely approximates a solid surface. Flow rate corresponds to 1–3% D \rightarrow C erosion yield over the holed surface area for typical low density, attached conditions in DIII-D, namely $\sim 1\text{--}7 \times 10^{17}$ CH₄ molecules/s (0.02 Torr L/s, ~ 2 sccm). Further details are provided in [2]. A DiMES TV picture of the PPI in CH/CD light, with puff on, is shown in Fig. 1.

The DIVIMP impurity production and transport code is 2D (poloidal/parallel and radial directions) [3]. The interpretation of DiMES impurity experiments requires 3D analysis and 3D-DIVIMP-HC has been developed from DIVIMP, including a hydrocarbon breakup module, and applied to the PPI experiments. 3D-DIVIMP-HC is a Monte Carlo modeling code which launches individual CH₄ molecules uniformly across the holed-portion of the DiMES surface. The particles are tracked in 3D as they experience the breakup processes tabulated in the Janev–Reiter (JR) [4,5] model/database. The simulation proceeds using a fixed time step, 10^{-9} s, which is chosen to be smaller than the characteristic times of any process which the particle experience.

* Corresponding author.

E-mail address: yrmu@starfire.utoronto.ca (Y. Mu).

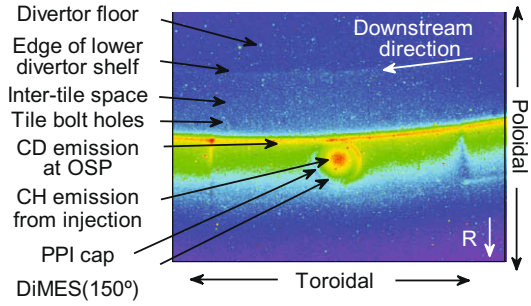


Fig. 1. DiMES TV view of the PPI in CH/CD light showing the light from the puff, at the center of DiMES. The bright arc at the upstream edge of the DiMES head is due to a slight vertical misalignment.

For charged particles (molecular ionic fragments, C^+ , etc.), the 3D motion is followed along the field lines allowing for diffusion (with imposed diffusion coefficients) in the radial and poloidal/dia-magnetic directions; parallel motion is governed by the friction force due to collisional-coupling with the background (fuel ion) plasma flow, the electric field force, as well as parallel diffusion (impurity pressure gradient force). These forces depend on back-ground plasma conditions which are input to the code based on measurements from Langmuir probes and divertor Thomson scattering. The electron and ion temperature gradient forces are not present in the case presented here due to the constant background plasma along the magnetic field lines being specified.

In addition to these general plasma forces there are also near-surface effects that need to be included. 3D-DIVIMP-HC includes a model for the magnetic pre-sheath (MPS) electric field from work by Brooks [6]. This electric field can be substantial in the near-surface region and can have a significant effect on loss of atomic and molecular ions from the plasma. In addition, 3D-DIVIMP-HC implements a range of surface interaction models for the hydrocarbon fragments. These options range from the ability to have all fragments stick to surfaces or reflect from surfaces. The experimental reflection coefficients from Jacob [7] were used here.

To make comparisons with spectroscopic measurements, the 3D spatially distributed emission of the atomic lines and molecular bands of interest are calculated based on the recorded density of each state. Photon emissivity coefficients from ADAS [8] for the atomic emission lines and HYDKIN [9] for the CH 0–0 band are used to calculate the emission from each cell of the modeling grid. The calculations here assumed that particles are in the ground state when excited by electron impact; this is not necessarily the case since molecular breakup can produce excited states; in future analysis this aspect will be further investigated. The total emission,

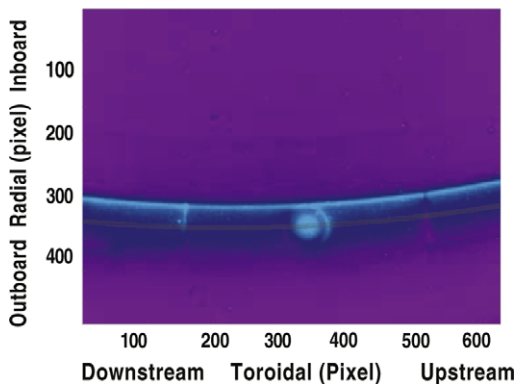


Fig. 2. CD/CH 2D TV picture with the toroidal arc region where the measured and calculated emission is compared (Fig. 4).

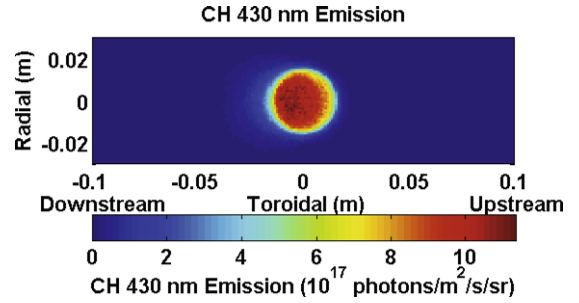


Fig. 3. CH 430 nm band emission 2D simulation from 3D-DIVIMP-HC.

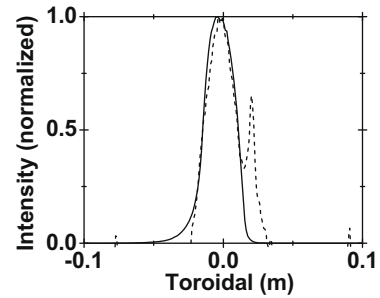


Fig. 4. CH comparison. Experiment: dot; code: solid. Shot #129689. The CH_4 was launched vertically with speed 650 m/s. $D_{\perp} = 0.3 \text{ m}^2/\text{s}$. The same simulation assumptions are used for Figs. 5 and 6. The spike at $T \sim 0.02 \text{ m}$, due to the misaligned upstream edge of the PPI, is evident in Figs. 4–6; this effect is not included in the present modeling.

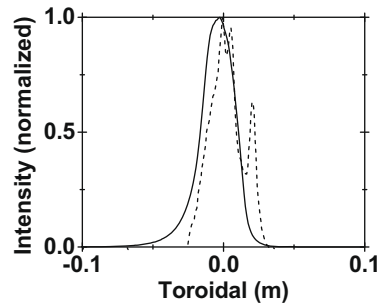


Fig. 5. Cl comparison. Experiment: dot; code: solid. Shot #129060. Other details as Fig. 4.

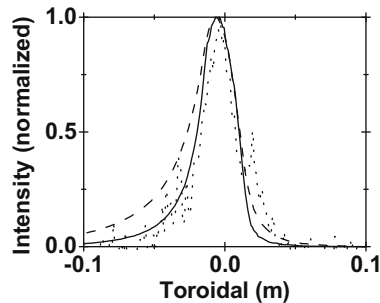


Fig. 6. CII comparison. Experiment: dot; code: solid (30 eV and $1.7 \times 10^{19} \text{ m}^{-3}$ background) and dash (20 eV and $1.2 \times 10^{19} \text{ m}^{-3}$ background). Shot #129691. Other details as Fig. 4.

Table 1Comparison of measured (MDS) and code-calculated absolute emissivities. Measurement uncertainties are a factor of ~ 2 .

	CH 427.0–431.5 nm	CI 909.0 nm	CII 426.7 nm	CII 514.0 nm	CII 658.0 nm
MDS L5 ($\times 10^{14}$ photons/cm ² /s/sr)	0.8	0.23	0.22	0.79	0.28
3D-DIVIMP-HC ($\times 10^{14}$ photons/cm ² /s/sr)	1.08	0.62	0.076	0.26	0.64

integrated along the required line-of-sight through the modeling grid is calculated and compared to the experimental value. The line-of-sight and viewing cone are chosen to match the experimental diagnostic.

2. Modeling and results

The 3D-DIVIMP-HC code was used to examine the CH, CI and CII emissions measured during the 2007 PPI experiment. This experiment was performed in an attached L-mode plasma with $T_e = 20$ – 30 eV and $n_e = 1.2$ – $1.7 \times 10^{19} \text{ m}^{-3}$ at the PPI location. We report here on (a) the spatial distribution of HC fragments and carbon particles, and (b) the absolute emission intensity of the following spectral measurements: CH 0–0 band, CI 909 nm and CII 427 nm, 514 nm and 658 nm. Data from four separate shots, found to be reproducible within the minimum range of error possible, were used to gather these data.

The CD/CH distribution measured by DiMES TV in shot #129689 is shown in Fig. 2. The edge of the PPI and the emission from the puffed CH₄ are clearly visible in the middle. In addition, emission coming from the strike point region where the plasma surface interaction is the strongest and at tile edges is clearly visible. There is also an observable emission from the upstream edge of DiMES due to a small misalignment of the sample holder. This makes it easy to correctly orient the images for comparison to the modeling results. The 3D-DIVIMP-HC simulation of the CH 430 nm band emission is shown in Fig. 3. This result models only the puffed CH₄ and so does not reproduce the band of naturally occurring emission corresponding to the strike point position or tile edges. In order to make quantitative comparisons of the toroidal profile through the center of the emission cloud, a toroidal arc (the black band in Fig. 2) composed of 8 pixels in the radial direction in the DiMES TV picture (~ 6 mm wide) is extracted, averaged and plotted against the 3D-DIVIMP-HC emission for the same region. In addition a background signal measured after the discharge is subtracted from the experimental profile prior to comparison. In Fig. 4, the 3D-DIVIMP-HC result (solid) is seen to match the measured profile (dot) fairly well.

The CI 909 nm distribution is measured by DiMES TV in shot #129060. The same process was applied to the analysis of this result as the CH measurement. The toroidal profile of this emission (dot) is then compared to the 3D-DIVIMP-HC results (solid) in Fig. 5. 3D-DIVIMP-HC matches experimental shape fairly well, although it appears to be somewhat narrower than the measured experimental profile. Due to the interaction at the upstream edge it is difficult to determine if the profile is just too narrow or just does not match the downstream tail of the CI profile. The CII distribution is measured by DiMES TV in shot #129691; in the downstream direction some of the CII emission from the puff is 'lost' due to the shadow in natural CII emission at the trailing edge gap of DiMES; to compensate, an increment has been added to the experimental. Toroidal profiles are compared in Fig. 6. There are several variables that affect the length of the tail. These include the efficiency of coupling the C⁺ to the background plasma flow as well as the effect of the MPS E-field and the radial and diamagnetic diffusion coefficients. All of these will affect the loss rate of carbon particles and the amount of time they have to couple to the back-

ground plasma flow. These dependencies are included in the model.

Absolute emission intensities of CH, CI 909 nm, CII 427 nm 514 nm and 658 nm were measured using MDS which views a 2.1 cm diameter circle centered on the DiMES sample. The particle source on DiMES is 3 cm across. As a result, the MDS views only regions which are the source of the puff. MDS background subtraction used the emission measured simultaneously on another MDS chord viewing at the same radial location but displaced toroidally. Comparisons with the code are shown in Table 1. The absolute magnitudes agree to within a factor of two for CH, CI and CII 658 nm emissions. The CII 427 nm and CII 514 nm emission modeling give results significantly below the experimental values. The possibility that the CII 427 nm line and the CII 514 nm line are due to excited C⁺ created by the CH₄ breakup is being investigated. The background plasma conditions used in the simulations are spatial averages of the Langmuir probe and divertor Thomson scattering measurements; however, ionization rates and photon efficiencies are fairly sensitive to the local plasma density and temperature. Thus, relatively small changes in the plasma conditions might have a significant effect on the absolute emissions as well as the ratios between the lines. This effect is also currently being investigated.

3. Conclusions

The Janev–Reiter methane breakup model/database, combined with the neutral and ionic transport modeling in the 3D-DIVIMP-HC code, successfully replicates a number of the major features of measurements made using the porous plug injection of CH₄ into an attached divertor plasma in DIII-D. It is therefore concluded that the most basic elements of the controlling physics and chemistry have been identified and incorporated in the code-modeling. A number of significant discrepancies between experiment and code-modeling have been identified and resolution of these differences is the focus of continuing experiment and code analysis.

Acknowledgments

This work was supported in part by the US Department of Energy under DE-FC02-04ER54698, DE-AC52-07NA27344, DE-FG02-07ER54917, and DE-AC04-94AL85000. The authors would like to acknowledge the DIII-D Team for their continued efforts in assisting our experiments and providing long time support, in particular, the DIII-D DiMES Group, including D.L. Rudakov, N.H. Brooks, C.P.C. Wong, and W.P. West. Support by the Natural Sciences and Engineering Research Council of Canada is acknowledged.

References

- [1] A.G. McLean et al., J. Nucl. Mater. 363–365 (2007) 86.
- [2] A.G. McLean et al., J. Nucl. Mater. 390–391 (2009) 160.
- [3] P.C. Stangeby, J.D. Elder, J. Nucl. Mater. 196–198 (1992) 258.
- [4] R.K. Janev, D. Reiter, Phys. Plasmas 9 (2002) 4071.
- [5] R.K. Janev, D. Reiter, J. Nucl. Mater. 313–316 (2003) 1202.
- [6] J. Brooks, Phys. Fluids B 2 (1990) 1858.
- [7] W. Jacob, J. Nucl. Mater. 337–339 (2005) 839.
- [8] H.P. Summers, The ADAS User Manual, Version 2.6, 2004. <<http://adas.phys.strath.ac.uk/>>.
- [9] D. Reiter. <<http://www.eirene.de/eigen/>>.